

**Clés, Code Liégeois d'Évolution Stellaire**  
Joint ENEAS and COROT Evolution and Seismic Tools Activity Workshop  
on Model Comparison, Aarhus, 24–28 October 2005

**Richard Scuflaire**  
Institut d'Astrophysique et de Géophysique de Liège

## Introduction

Since the early 70s, our research group at the Institute of Astrophysics of Liège has been using an evolution code derived from the Henyey code. This code has been continuously updated. Nevertheless, with the progress of asteroseismology, it became clear that the frequencies and the stability of the oscillation modes were too sensitive to details of the model, which were unimportant for the computation of stellar evolution. It was thus decided to write a new code, meeting the specific requirements of our studies in asteroseismology. This code has been named *Clés*. It is the acronym for *Code Liégeois d'Évolution Stellaire*. It is still in an active phase of development. The code is intended to be easily customized to the needs of the user.

In the presentation of *Clés* I made at the ESTA meeting in Nice (Scuflaire, 2005) I insisted on the differences between *Clés* and CESAM and J. Montalbán and Y. Lebreton (2005) compared evolutions computed by these codes, after having brought the physics of both codes closer to each other. The computed evolutions turned out to be in very good agreement, though both codes rely on completely different numerical approaches.

In the present talk, I will briefly describe some features of the current version of *Clés* (version 18) and say a few words about the developments in progress. I will emphasize a few points which are probably not very important by themselves but which cannot be neglected in detailed comparisons of evolution codes: the adopted values of the physical constants and the ambiguities in the definition of the standard GN93 mixture.

## Numerics

*Clés* is a lagrangian code. Finite difference equations of order two are used for the discretization of the spatial equations. The mesh is automatically adapted so as to limit the variations of physical variables from one point to the next one. The default criteria used to choose the mesh size are

$$\Delta r/R \leq 5 \times 10^{-3}, \quad \Delta m/M \leq 5 \times 10^{-3}, \quad \Delta P/P \leq 5 \times 10^{-2} \quad \text{and} \quad \Delta T/T \leq 10^{-2}.$$

Unfortunately, no effort has been made to increase the number of points near the boundaries of convective zones. With these criteria, a  $2 M_{\odot}$  model starts its evolution on the Hayashi track with 700 points and reaches the zero-age main sequence with 1150 points.

The same total number of points is approximately kept along the main sequence, with local additions or deletions of points. A simple command allows the user to require a finer or a coarser mesh.

The finite difference scheme written to follow the time evolution of the abundances is of order one to avoid numerical instabilities. The timestep is chosen to limit the variations of the physical variables from one model to the next. For instance, for a  $2 M_{\odot}$  model in its PMS or MS phases, the following default limitations are imposed on the variations of the physical variables from one model to the next.

	$\Delta T/T$	$\Delta P/P$	$\Delta T_e/T_e$	$\Delta L/L$	$\Delta X_c$
if $T_c \leq 1.6 \times 10^7$	$4.0 \times 10^{-1}$	$5.0 \times 10^{-1}$	$4.0 \times 10^{-2}$	$1.0 \times 10^{-1}$	$1.0 \times 10^{-2}$
if $T_c > 1.6 \times 10^7$	$5.0 \times 10^{-2}$	$7.0 \times 10^{-2}$	$7.0 \times 10^{-3}$	$3.0 \times 10^{-2}$	$1.0 \times 10^{-2}$

The evolution sequences are normally started on the Hayashi sequence. With the above criteria, a  $2 M_{\odot}$  model evolution needs 125 steps for the pre-main sequence, 75 steps for the main sequence and 20 steps for the second gravitational contraction.

The timestep may be increased or decreased according to the needs of the user. It is also automatically reduced when the resolution of the spatial equations becomes too slow.

## Equation of state

Two equations of state (EOS) are implemented, CEFF (Christensen-Dalsgaard and Däppen 1992) and OPAL 2001 (Rogers et al. 1996, Rogers 2001). OPAL comes in tabular form, but tables have also been built for the CEFF EOS (to accelerate the computations). We were not satisfied with the OPAL interpolation routines. We use our own interpolation routines which ensure the continuity of the first derivatives at cell boundaries in the four-dimensional space defined by the variables  $\log \rho$ ,  $\log T$ ,  $X$  and  $Z$ . The detailed metal mixture is supposed to be unimportant for the EOS (and cannot be changed for OPAL).

J. Montalban and Y. Lebreton (2005) have shown how the inconsistencies in the OPAL thermodynamic quantities, first pointed out by Boothroyd and Sackmann (2003), may affect the comparison of evolution sequences computed by different evolution codes.

## Opacity

Clés uses the OPAL opacities (Iglesias and Rogers 1996), completed with the opacities of Alexander and Ferguson (1994) at low temperature. The tables are merged in a smooth way. In the temperature domain  $\log T \in [3.9, 4.15]$  where the opacity is defined in both tables, Clés uses an opacity  $\kappa$  defined as the average

$$\log \kappa = (1 - \theta) \log \kappa_{AF} + \theta \log \kappa_{OPAL},$$

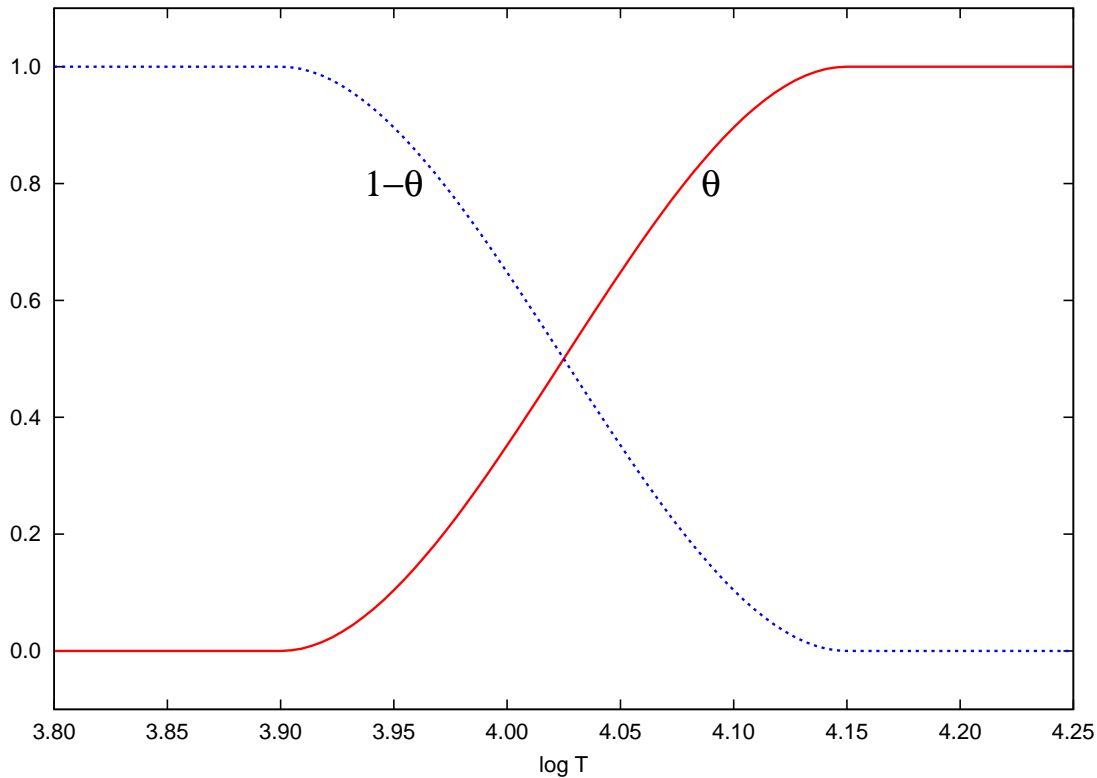


Figure 1: The opacities of Alexander and Ferguson (1994) and OPAL are merged using the function  $\theta$ .

where  $\theta$  is the third degree polynomial in  $\log T$  illustrated in Fig 1.

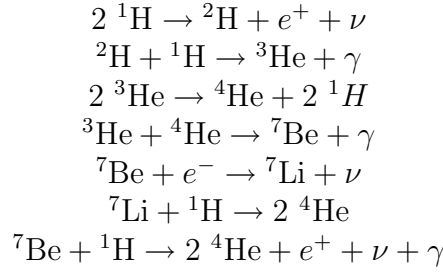
Again we use our own interpolation routines in the four variables  $\log R$ ,  $\log T$ ,  $X$  and  $Z$ , where  $R = \rho/T_6^3$ . At the present time, the metal mixture is fixed for the computation of the opacity, within a given model. A few tables are available for different metal mixtures and new tables are easily computed.

I will discuss later how the ambiguity about the widely used GN93 metal mixture can affect the opacities.

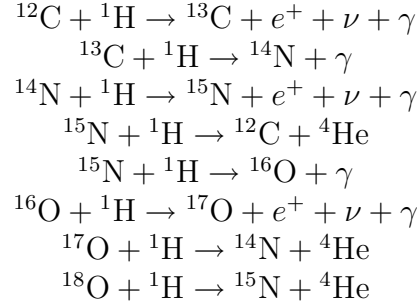
## Nuclear energy generation

The following reactions are taken into account in Clés.

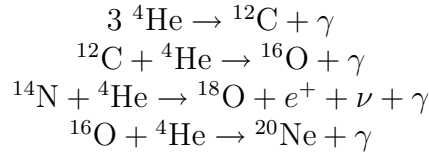
p-p chains:



CNO cycles:



He combustion:



We follow thoroughly the combustion of  $^2\text{H}$  and  $^7\text{Li}$ . Only unstable species (as  $^7\text{Be}$ ,  $^{13}\text{N}$ ,  $^{15}\text{O}$  and  $^{17}\text{F}$ ) are supposed to be at equilibrium.

We have already implemented the main reactions of the helium burning phase but we have yet to improve our code to be able to accurately follow this phase of the evolution (semi-convection, equation of state, opacity).

The Caughlan and Fowler (1988) reaction rates have been used. For  $^{14}\text{N}(p,\gamma)^{15}\text{O}$ , we use the significantly lower cross-section given by Formicola et al. (2004). A variant of the program using the NACRE reaction rates in their approximate analytical form (Angulo et al. 1999) has been written to facilitate the comparisons with CESAM.

The next version of Clés will use NACRE tables instead of analytical fits.

Detailed comparisons between Clés and CESAM showed that the screening factors were slightly different (a few  $10^{-4}$  to  $10^{-3}$ ) though both programs implemented the Salpeter (1954) formula.

$$f = \exp\left(0.188Z_1Z_2\sqrt{\frac{\zeta\rho}{T_6^3}}\right) \quad \text{with} \quad \zeta = \sum_i Z_i(Z_i + 1)\frac{X_i}{A_i}.$$

It turned out that a large part of the differences could be ascribed to the value of the coefficient adopted in Clés (it has been recomputed with recent values of the physical

constants and is taken as 0.18791 instead of 0.188) and in an approximation in the computation of  $\zeta$  (which was computed with the assumption of a GN93 metal mixture). See J. Montalban (2005, this workshop) for more details.

## Gravitational energy generation

There are two different versions of this term in textbooks. In Cox and Giuli (1968) for instance, we find

$$\epsilon_g = -T \frac{dS}{dt} - \sum_i \mu_i \frac{dn_i}{dt},$$

where the  $\mu_i$  are the chemical potentials and the  $n_i$  the number of moles per gram. In Kippenhahn and Weigert (1990) we find

$$\epsilon_g = -T \frac{dS}{dt}.$$

The difference between both expressions is not negligible. If we integrate during the whole main sequence, the difference is of the order of the local internal energy. There is a very convincing paper of Strittmatter et al. (1970) in favor of the first expression, which can also be written

$$\epsilon_g = \frac{dU}{dt} - P \frac{d(1/\rho)}{dt}.$$

We have adopted this form of  $\epsilon_g$  in the current version of Clés.

## Convection

We have implemented the usual mixing-length theory of Böhm-Vitense (1958), also exposed in the textbooks of Cox and Giuli (1968) and Kippenhahn and Weigert (1990).

In a convective zone, it is usual to define four gradients:  $\nabla_{rad} > \nabla > \nabla' > \nabla_{ad}$ . To determine  $\nabla$  in terms of  $\nabla_{rad}$  and  $\nabla_{ad}$ , one must solve a cubic equation in  $\Gamma$ , the efficiency of convection (defined as the ratio of the energy effectively transported by convective elements to the energy they lose by radiation). In the Böhm-Vitense theory, this equation reads

$$\frac{9}{4}\Gamma^3 + \Gamma^2 + \Gamma = B(\nabla_{rad} - \nabla_{ad}),$$

where the mixing-length parameter enters the definition of coefficient  $B$ . Each term of the left-hand side of this equation is linked to a gradient difference,

$$\frac{9}{4}\Gamma^3 = B(\nabla_{rad} - \nabla), \quad \Gamma^2 = B(\nabla - \nabla'), \quad \Gamma = B(\nabla' - \nabla_{ad}).$$

From these relations the actual gradient in the convective zone can be expressed as

$$\nabla = \frac{\frac{9}{4}\Gamma^2 \nabla_{ad} + (\Gamma + 1) \nabla_{rad}}{\frac{9}{4}\Gamma^2 + \Gamma + 1}.$$

The usual prescription for the choice of the mixing-length  $\ell$  is

$$\ell = \alpha H_P,$$

where  $H_P$  is the pressure scale height and  $\alpha$  a coefficient, the value of which is determined by a solar calibration (the value we determine in this way is of the order of 1.8).

Heney et al. (1965) have described a variant which has been totally or partially implemented in some evolution codes, but not in ours.

Presently, the mesh is not adapted to a rigorous treatment of the boundaries of the convective zones. This results in some *numerical diffusion* at the boundaries. This does not seem to be a major problem but we plan to better describe these boundaries with double mesh points in a future version of the code.

## Overshooting

In the present version of Clés, the extension of the overshooting zone is limited in a rather conventional way

$$r_{ov} = r_c \pm \alpha_{ov} \min(H_P, h),$$

where  $r_c$  is the radius at the boundary of the convective zone and  $h$  its size.

In the standard version of Clés, the gradient in overshooting zones is taken as the radiative gradient  $\nabla_{rad}$ , whereas in other codes it is taken as the adiabatic gradient  $\nabla_{ad}$ . However, one of our PhD student, Mélanie Godard, with the help of Josefina Montalban, has also implemented the possibility of a choice between the two gradients. This will allow comparisons with other evolution codes.

## Diffusion

We follow the theory of stellar diffusion developed by Thoul et al. (1994). A rather crude treatment taking into account only three components (H, He and metals) and neglecting the radiative forces is presently implemented. Pierre-Olivier Bourge, one of our PhD student, in collaboration with Georges Alecian, is implementing a more detailed treatment taking radiative forces into account in a particular version of the code.

## Atmosphere

The models computed by Clés extend up to the photosphere ( $T = T_e$ ) or an optical depth  $\tau = 1, 10$  or  $100$  chosen by the user where they are fitted to a model atmosphere of Kurucz with overshooting (1998). A grey Eddington atmosphere (without convection) can also be fitted at the photospheric level.

## The GN93 mixture

Table 1 shows the origin of the metal abundances used in OPAL opacities. In a first step, the 23 most abundant metals (from Li to Ni) have been retained. The values adopted by OPAL come from three publications: Anders and Grevesse (1989), Grevesse and Noels (1993) and Grevesse and Sauval (1998). This last publication is more recent than the Iglesias and Rogers (1996) publication, but private communications have been exchanged. The normalized number abundances of this 23 elements mixture are given in column  $f_{23}$  of the table. In a second step the abundances of the 4 less abundant metals in this list (F, Sc, V and Co) have been redistributed between their neighbours in the table, reducing the list to 19 elements (column  $f_{19}$  of the table).

The precomputed GN93 OPAL opacity table is so widely used for stellar evolution studies that probably GN93 means the values in the  $f_{19}$  column.

Another feature of the GN93 OPAL opacity tables is the choice of atomic masses. Table 2 shows the mean atomic masses (column AG89) computed from the isotopic abundances of Anders and Grevesse (1989) and recent atomic masses (Audi et al. 2003) and the values adopted for the computation of OPAL opacities. The agreement is generally good enough, except for Ar where the difference amounts to 10 %. The effects of this difference on the opacities have been discussed by J. Montalban (2005, this workshop).

A third remark about the GN93 mixture concerns the abundances of Li, Be, B. In the current version of Clés, we follow the abundance of  $^7\text{Li}$  and in the version in development we will follow the evolution of  $^6\text{Li}$ ,  $^7\text{Li}$ ,  $^9\text{Be}$ ,  $^{10}\text{B}$  and  $^{11}\text{B}$ . So we need initial abundances. Because of the possibility of partial nuclear processing of these elements in the Sun, we prefer to adopt their meteoritic values (contrary to the case of the other metals). Table 3 gives the meteoritic and photospheric abundances of these elements according to Anders and Grevesse (1989) and Grevesse and Noels (1993).

With these three remarks, I wanted to stress the ambiguity of the definition of the GN93 metal mixture. This term has certainly not the same meaning for everybody, as was shown by J. Montalban (2005, this workshop). It does not define the abundances of the elements in a unique way and must be completed by isotopic abundances.

Table 1: The GN93 mixture as used in OPAL opacities,  $\log A$  refers to logarithmic abundances in an arbitrary scale while  $f$  refers to normalized (sum = 1) number abundances.

		log A				number abundance	
		AG89	GN93	GS98	OPAL	$f_{23}$	$f_{19}$
6	C	8.56	<span style="border: 1px solid blue; padding: 1px;">8.55</span>	8.52	8.55	2.45518e-1	2.45518e-1
7	N	8.05	<span style="border: 1px solid blue; padding: 1px;">7.97</span>	7.92	7.97	6.45777e-2	6.45777e-2
8	O	8.93	<span style="border: 1px solid blue; padding: 1px;">8.87</span>	8.83	8.87	5.12959e-1	<span style="border: 1px solid red; padding: 1px;">5.12966e-1</span>
9	F	<span style="border: 1px solid blue; padding: 1px;">4.56</span>		4.56	4.56	2.51236e-5	
10	Ne	8.09	8.07	<span style="border: 1px solid blue; padding: 1px;">8.08</span>	8.08	8.31922e-2	<span style="border: 1px solid red; padding: 1px;">8.32102e-2</span>
11	Na	<span style="border: 1px solid blue; padding: 1px;">6.33</span>		6.33	6.33	1.47939e-3	1.47939e-3
12	Mg	<span style="border: 1px solid blue; padding: 1px;">7.58</span>		7.58	7.58	2.63077e-2	2.63077e-2
13	Al	<span style="border: 1px solid blue; padding: 1px;">6.47</span>		6.47	6.47	2.04213e-3	2.04213e-3
14	Si	<span style="border: 1px solid blue; padding: 1px;">7.55</span>		7.55	7.55	2.45518e-2	2.45518e-2
15	P	<span style="border: 1px solid blue; padding: 1px;">5.45</span>		5.45	5.45	1.95022e-4	1.95022e-4
16	S	<span style="border: 1px solid blue; padding: 1px;">7.21</span>		7.33	7.21	1.12223e-2	1.12223e-2
17	Cl	<span style="border: 1px solid blue; padding: 1px;">5.50</span>		5.50	5.50	2.18818e-4	2.18818e-4
18	Ar	6.56	6.60	6.40	6.52	2.29130e-3	2.29130e-3
19	K	<span style="border: 1px solid blue; padding: 1px;">5.12</span>		5.12	5.12	9.12184e-5	9.12184e-5
20	Ca	<span style="border: 1px solid blue; padding: 1px;">6.36</span>		6.36	6.36	1.58519e-3	<span style="border: 1px solid red; padding: 1px;">1.58558e-3</span>
21	Sc	3.10	3.14/3.20	<span style="border: 1px solid blue; padding: 1px;">3.17</span>	3.17	1.02349e-6	
22	Ti	4.99	5.03/5.04	<span style="border: 1px solid blue; padding: 1px;">5.02</span>	5.02	7.24574e-5	<span style="border: 1px solid red; padding: 1px;">7.48770e-5</span>
23	V	<span style="border: 1px solid blue; padding: 1px;">4.00</span>		4.00	4.00	6.91963e-6	
24	Cr	<span style="border: 1px solid blue; padding: 1px;">5.67</span>		5.67	5.67	3.23655e-4	<span style="border: 1px solid red; padding: 1px;">3.28793e-4</span>
25	Mn	<span style="border: 1px solid blue; padding: 1px;">5.39</span>		5.39	5.39	1.69857e-4	1.69857e-4
26	Fe	7.67	7.51	<span style="border: 1px solid blue; padding: 1px;">7.50</span>	7.50	2.18818e-2	<span style="border: 1px solid red; padding: 1px;">2.18771e-2</span>
27	Co	<span style="border: 1px solid blue; padding: 1px;">4.92</span>		4.92	4.92	5.75549e-5	
28	Ni	<span style="border: 1px solid blue; padding: 1px;">6.25</span>		6.25	6.25	1.23050e-3	<span style="border: 1px solid red; padding: 1px;">1.29276e-3</span>

Table 2: Atomic masses computed from Anders and Grevesse (1989) isotopic abundances and atomic masses adopted by OPAL.

		AG89	OPAL	diff.
1	H	1.007859	1.00790	
2	He	4.002463	4.00260	
6	C	12.011037	12.01100	
7	N	14.006723	14.00670	
8	O	15.999305	15.99940	
10	Ne	20.130472	20.17900	0.2 %
11	Na	22.989770	22.98977	
12	Mg	24.305052	24.30500	
13	Al	26.981538	26.98154	
14	Si	28.085509	28.08550	
15	P	30.973762	30.97376	
16	S	32.064388	32.06000	
17	Cl	35.452738	35.45300	
18	Ar	36.282786	39.94800	10.1 %
19	K	39.098301	39.09830	
20	Ca	40.078023	40.08000	
22	Ti	47.878426	47.90000	
24	Cr	51.996138	51.99600	
25	Mn	54.938050	54.93800	
26	Fe	55.846819	55.84700	
28	Ni	58.687892	58.70000	

Table 3: Meteoritic and photospheric abundances of Li, Be and B.

		log A (AG89, GN93)	
		meteor.	phot.
3	Li	3.31	1.16
4	Be	1.42	1.15
5	B	2.88	2.60

## References

- D.R. Alexander, J.W. Ferguson, 1994, *ApJ*, 437, 879–891.
- E. Anders, N. Grevesse, 1989, *Geochimica and Cosmochimica Acta*, 53, 197–214.
- C. Angulo et al., 1999, *Nuclear Physics A*, 656, 3–183.
- G. Audi, A.H. Wapstra and C. Thibault, 2003, *Nuclear Physics A*, 729, 337–676.
- E. Böhm-Vitense, 1958, *Z. Astrophysik*, 46, 108–143.
- A.I. Boothroyd, I.-J. Sackmann, 2003, *ApJ*, 583, 1004–1023.
- G.R. Caughlan, W.A. Fowler, 1988. *Atomic data and nuclear tables*, 40, 283–334.
- J. Christensen-Dalsgaard, W. Däppen, 1992, *A&A*, 4, 267–361.
- J.P. Cox, R.T. Giuli, 1968, *Principles of stellar structure*, Gordon and Breach.
- A. Formicola et al., 2004, *Physics Letters B*, 591, 61–68.
- N. Grevesse, A. Noels, 1993, in *Origin and evolution of the elements*, eds N. Pratzko, E. Vangioni-Flam, M. Cassé, Cambridge University Press, p 15–25.
- N. Grevesse, A.J. Sauval, 1998, in *Solar composition and its evolution from core to corona*, workshop held at ISSI (Bern).
- L. Henyey, M.S. Vardya, P. Bodenheimer, 1965, *ApJ*, 142, 841–854.
- C.A. Iglesias, F.J. Rogers, 1996, *ApJ*, 464, 943–953.
- R. Kippenhahn, A. Weigert, 1990, *Stellar structure and evolution*, Springer-Verlag.
- R.L. Kurucz, 1998, <http://kurucz.harvard.edu/grids.html>.
- J. Montalban, 2005, ESTA Meeting 4, Aarhus, 24–28 October 2005,  
[http://www.astro.up.pt/corot/welcome/meetings/m4/ESTA\\_Aarhus\\_Montalban.pdf](http://www.astro.up.pt/corot/welcome/meetings/m4/ESTA_Aarhus_Montalban.pdf)
- J. Montalban, Y. Lebreton, ESTA Meeting 3, Nice, 26–27 September 2005,  
[http://www.astro.up.pt/corot/welcome/meetings/m3/ESTA\\_Nice\\_Montalban.pdf](http://www.astro.up.pt/corot/welcome/meetings/m3/ESTA_Nice_Montalban.pdf)
- F.J. Rogers, 2001, *Contributions to plasma physics*, 41, 179–182.
- F.J. Rogers, F.J. Swenson, C.A. Iglesias, 1996, *ApJ*, 456, 902–908.
- E.E. Salpeter, 1954, *Austral. J. Phys.*, 7, 373–388.
- R. Scuflaire, 2005, ESTA Meeting 3, Nice, 26–27 September 2005,  
[http://www.astro.up.pt/corot/welcome/meetings/m3/ESTA\\_Nice\\_Scuflaire\\_1.pdf](http://www.astro.up.pt/corot/welcome/meetings/m3/ESTA_Nice_Scuflaire_1.pdf)
- P.A. Strittmatter, J. Faulkner, J.W. Robertson, D.J. Faulkner, 1970, *ApJ*, 161, 369.
- A. Thoul, J.N. Bahcall, A. Loeb, 1994, *ApJ*, 421, 828–842.